

# Comparative study of geometry and bonding character for methoxy radical adsorption on noble metals

J.R.B. Gomes, J.A.N.F. Gomes\*

CEQUP/Departamento de Química, Faculdade de Ciências, Universidade do Porto, Rua do Campo Alegre, 687, 4169-007 Porto, Portugal

Received 19 April 1999; received in revised form 13 July 1999; accepted 26 July 1999

## Abstract

Results are reported of quantum density functional theory (DFT) calculations for methoxy radical adsorption on the (111) surfaces of copper, silver and gold. The metallic surfaces are modeled by clusters of seven atoms chosen to simulate the top, bridge, hcp hollow and fcc hollow sites. A control test on the use of these small clusters was performed by running a calculation on a 22-atoms cluster. A comparison between the energetics of adsorption on the different sites identifies the fcc hollow position as the preferred one for  $\text{CH}_3\text{O}$  adsorption on the metal surfaces considered and the methoxy C–O axis is found to be perpendicular to the surface. It is shown how the methoxy radical binds on the hollow sites of copper, silver and gold metallic surfaces; the three oxygen p orbitals are found to interact strongly with the nearest neighbour metallic atoms except for the top position where only the p orbital aligned along the direction of the oxygen–metal atom is involved. In all cases, there is a charge transfer of approximately 0.6–0.8e from the metal atoms to the methoxy radical. The bonding of the methoxy radical on the surfaces studied has a largely ionic character. The calculated adsorption parameters and vibrational frequencies of the adsorbed species are in good agreement with the available experimental data. © 2000 Elsevier Science B.V. All rights reserved.

**Keywords:** Density functional theory; Transition metal surfaces;  $\text{CH}_3\text{O}^\cdot$ ; Chemisorption; Vibrations of adsorbed molecules; Methanol oxidation

## 1. Introduction

Over the last two decades, there has been considerable interest in the chemistry of methanol on transition metal surfaces, inspired in part by the use of copper as a catalyst in methanol synthesis [1–4]. In addition, the fact that methanol reactions are capable of forming stable surface intermediates makes these reactions attractive to study by a diversity of surface techniques.

The adsorption and decomposition of methanol have been investigated on a variety of metal surfaces,

for example, Cr(110) [5], Ni(100) [6], Ni(110) [7], Ni(111) [8], Cu(100) [9–11], Cu(110) [12–14], Cu(111) [15–18], Ag(110) [19,20], Ag(111) [21], Au(110) [22], Pd(110) [23], Pd(111) [24], Pt(100) [25], Pt(110) [26], Mo(100) [27], Mo(110) [28] and Al(111) [29]. In all these surfaces, the methoxy radical,  $\text{CH}_3\text{O}^\cdot$ , is the dominant surface intermediate at temperatures below 350 K, being easily formed by cleavage of the O–H bond of methanol. The product distribution observed during the thermal decomposition varies with the nature of the surface and with the presence or absence of pre-adsorbed oxygen. This is due to the great dependence of the methoxy fragment reactivity on the surface orientation of the metal.

Bowker and co-workers [13,14] have studied the adsorption and the partial oxidation of methoxy on

\* Corresponding author. Tel.: + 351-2-6082807; fax: + 351-2-6082959.

E-mail address: jfgomes@fc.up.pt (J.A.N.F. Gomes).

Cu(110) using temperature programmed desorption (TPD), low energy electron diffraction (LEED) and scanning tunneling spectroscopy (STM) [14]. At a temperature below 200 K, there is the formation of adsorbed  $\text{CH}_3\text{O}^\cdot$  owing to the decomposition of  $\text{CH}_3\text{OH}$  by O–H bond cleavage. At 350 K, desorption of formaldehyde, hydrogen and some methanol is observed experimentally and, at 440 K, small amounts of  $\text{CO}_2$  evolve from the Cu(110) surface.

Methanol adsorbs on clean and oxidized copper(111) at 91 K. On the clean surface  $\text{CH}_3\text{OH}$  is completely desorbed while on the oxidized surface a deprotonation reaction takes place resulting in the production of the methoxy species. This intermediate was found by Chesters et al. [18] to be adsorbed with a  $\text{C}_{3v}$  symmetry.

In adsorption studies of  $\text{CH}_3\text{OH}$  on Ag(111) [21] and on Au(110) [22],  $\text{CH}_3\text{O}^\cdot$  is also found as a stable intermediate. The formation of methyl formate and water at 250 K on Au(110) and  $\text{CO}_2$  at 340 K has been observed. On Ag(111) there is formation of  $\text{CH}_3\text{O}^\cdot$  at 180 and at 290 K  $\text{H}_2\text{CO}$  and  $\text{H}_2$  evolve. Small amounts of formate were detected at approximately 220 K and at 350 K there is  $\text{CO}_2$  desorption. Surprisingly,  $\text{H}_2\text{CO}$  is not a product of methanol oxidation on Au(110), while it is the principal product on Cu(110) and Ag(110) surfaces as well as on the other copper and silver low index surfaces. It has been proposed that formaldehyde react with methoxy to yield methyl formate [22]. A tilted orientation for the molecular axis of  $\text{CH}_3\text{O}$  radical was found for adsorption on Cu(110) [30,31]. X-ray photoelectron diffraction (XPD) [17] studies for  $\text{Cu}(111)\text{OCH}_3$  and reflection absorption infrared spectroscopy (RAIRS) [21] for  $\text{Ag}(111)\text{OCH}_3$ , showed that the  $\text{CH}_3\text{O}$  radical resides in the 3-fold hollow site and that the CO bond axis is normal to the surface plane.

Some theoretical studies have also been done on the methoxy–metal surface interactions [16,32,33]. A many-electron embedding theory, at the ab initio configuration interaction level, was used to study the adsorption of methoxy on the Ni(111) surface [32]. That work showed how  $\text{CH}_3\text{O}^\cdot$  is adsorbed at 3-fold hollow sites with the C–O axis tilted  $5^\circ$  from the normal to the surface plane and bound to Ni(111) mainly via its  $5a_1$ ,  $1e$  and  $2e$  orbitals. Witko et al. [16,33] have studied the adsorption of  $\text{CH}_3\text{O}^\cdot$  on Cu(111) by performing ab initio HF-LCAO calcula-

tions. Again it was found that  $\text{CH}_3\text{O}^\cdot$  is usually adsorbed at 3-fold hollow sites with a slight preference for fcc sites. On Cu(111), the C–O axis lies perpendicular to the metal surface and the calculated adsorption energy is 270 kJ/mol.

Despite the existence of a large number of studies, conflicting structural assignments still exist. The near-edge X-ray absorption fine structure (NEXAFS) study of Outka et al. [34] shows that methoxy C–O axis will be found with an angle of  $20\text{--}40^\circ$  relative to the Cu(100) surface normal. Using the infrared spectroscopy [2,35], Ryberg also found that methoxy is tilted when adsorbed on this surface. Camplin et al. [11], using the RAIRS technique, found the C–O methoxy radical bond to be perpendicular to the Cu(100) surface. A later study of Lindner et al. [36] with a combined NEXAFS and photoelectron research concluded that the C–O axis is perpendicular to the surface and that a low symmetry adsorption site between the bridge and the 4-fold hollow site is occupied.

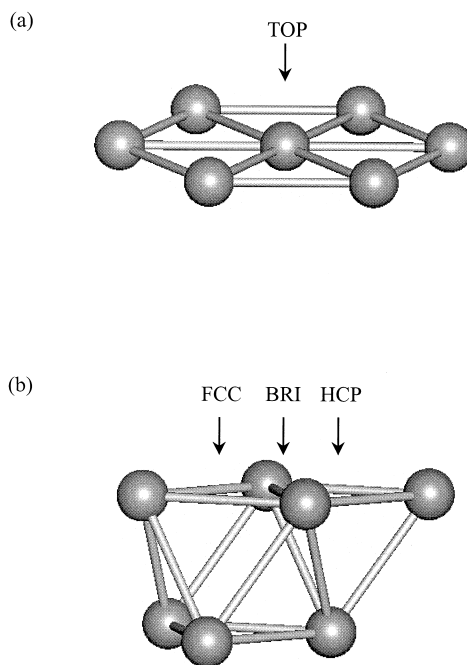


Fig. 1. Representation of adsorption sites on  $\text{M}_7$  clusters with  $\text{M} = \text{Cu}, \text{Ag}$  and  $\text{Au}$ . Arrows represent the oxygen atom of the methoxy radical. (a) Cluster used for  $\text{CH}_3\text{O}$  adsorption study on a top site and (b) cluster used for  $\text{CH}_3\text{O}$  adsorption study on a bridge site and on hollow sites.

In this contribution, the adsorption of  $\text{CH}_3\text{O}^\cdot$  on the Cu, Ag and Au(111) surfaces is described by means of the density functional theory (DFT). The goals were to study the energetics of  $\text{CH}_3\text{O}^\cdot$  adsorption and compare the chemisorptive properties of the radical on metallic clusters as a function of surface site, cluster size and noble metal element. The calculated values are compared with experimental data available, in order to test the validity of our approximations.

This paper is organized as follows. In Section 2, we briefly outline the theoretical details of the cluster calculations including the geometry and the number of metal atoms used to model the metal surface, the methoxy radical internal geometry, the theoretical method used in the calculations of the chemisorptive properties and basis sets. The numerical results obtained for the adsorption parameters and vibrational frequencies are presented and discussed in Section 3. Finally in Section 4, a summary of the major conclusions is presented.

## 2. Method

In the present work, the methoxy radical interaction with copper, silver and gold(111) surfaces is studied. The system is modeled by clusters of the type  $\text{M}_n\text{OCH}_3$  composed of seven metal atoms. The  $\text{M}_7$  substrate clusters are chosen as sections of the ideal M(111) surface where the bulk value for M–M nearest neighbor distance are, in Å, 2.551 for Cu, 2.888 for Ag and 2.883 for Au. The clusters used in this study are shown in Fig. 1. The hollow sites that appear in the M(111) surface are 3-fold sites labeled fcc and hcp which differ by the position of the atoms in the second layer (on the hcp site there is a metallic atom directly underneath it in the second layer and on the fcc site the central metallic atom is repeated in the third layer). Obviously, for the clusters that have only one layer the fcc and hcp labels are irrelevant. The other adsorption sites of methoxy considered here were the bridge position, when the oxygen atom is positioned above an M–M bond, and the top position when the oxygen

Table 1

Methoxy adsorption properties for the different  $\text{Cu}_7$  clusters representing on-top, bridge and hollow sites.  $E_a$  is the methoxy adsorption energy,  $d(\text{O}-\text{Cu}_{\text{surf}})$  is the perpendicular distance to the copper surface,  $d(\text{O}-\text{Cu}_m)$  is the distance between the methoxy oxygen atom and the nearest Cu atom(s) on the surface,  $d(\text{O}-\text{C})$  is the length of the C–O bond.  $\angle(\text{O}-\text{C}-\text{H})$  and  $\angle(\text{Cu}_{\text{nor}}-\text{O}-\text{C})$  are, respectively, the angle between the CO and CH bonds and the angle of CO bond with respect to the surface normal (see Fig. 2).  $q(\text{adsorbate})$  is the total charge on the adsorbate in a.u. computed by Natural Population Analysis [47]. Frequencies are in  $\text{cm}^{-1}$

Cu(111)	Top	Top tilted	Bridge	Bridge tilted	hcp	fcc	Experimental
$E_a/\text{kJ mol}^{-1}$	–155.6	–177.0	–196.4	–202.7	–210.6	–241.4	
$d(\text{O}-\text{Cu}_{\text{surf}})/\text{Å}$	1.937	1.977	1.568	1.590	1.461	1.457	$1.32 \pm 0.05^b$
$d(\text{O}-\text{Cu}_m)/\text{Å}$	1.937	1.977	2.021	2.039	2.075	2.072	$1.98 \pm 0.03^b$
$d(\text{O}-\text{C})/\text{Å}$	1.375	1.368	1.405	1.411	1.413	1.406	$1.42 (-0.03/ + 0.10)^b$
$\angle(\text{O}-\text{C}-\text{H})^\circ$	113.1	113.6	111.6	111.6	111.1	111.3	
$\angle(\text{Cu}_{\text{nor}}-\text{O}-\text{C})^\circ$	0.0	53.1	0.0	30.1	0.0	0.0	$0.0^{\text{c,d}}$
$q(\text{adsorbate})$	–0.82	–0.77	–0.75	–0.73	–0.74	–0.76	
$\nu_{\text{as}}(\text{CH}_3)$	2830	2840	2881	2868	2891	2884	$2888^{\text{c}}/2922^{\text{e}}$
$\nu_{\text{as}}(\text{CH}_2)$	2830	2821	2877	2885	2889	2883	
$\nu_{\text{s}}(\text{CH}_3)$	2808	2749	2829	2825	2833	2831	$2818^{\text{d}}/2808^{\text{e}}$
$\delta_{\text{as}}(\text{CH}_3)$	1440	1441	1456	1448	1458	1460	$1464^{\text{e}}$
$\delta_{\text{as}}(\text{CH}_2)$	1439	1374	1450	1455	1458	1453	
$\delta_{\text{s}}(\text{CH}_3)$	1442	1421	1446	1441	1444	1447	$1435^{\text{e}}$
$\rho(\text{CH}_3)$	1125	1106	1147	1141	1144	1148	$1150^{\text{e}}$
$\rho(\text{CH}_2)$	1124	1078	1135	1135	1150	1148	
$\nu(\text{CO})$	1156	1134	1098	1064	1075	1101	$1036^{\text{d}}/1039^{\text{e}}$
$\nu(\text{OCu}_{\text{surf}})$	358	408	360	370	355	360	$328^{\text{e}}$

<sup>a</sup> Negative values are exothermic.

<sup>b</sup> Backscattering Photoelectron experiments, Ref. [15].

<sup>c</sup> XPD value, Ref. [17].

<sup>d</sup> FT-RAIR values, Ref. [18].

<sup>e</sup> EELS values, Ref. [16].

Table 2

Methoxy adsorption properties for the different  $\text{Ag}_7$  clusters representing on-top, bridge and hollow sites.  $E_a$  is the methoxy adsorption energy,  $d(\text{O}-\text{Ag}_{\text{surf}})$  is the perpendicular distance to the copper surface,  $d(\text{O}-\text{Ag}_{\text{nm}})$  is the distance between the methoxy oxygen atom and the nearest Ag atom(s) on the surface,  $d(\text{O}-\text{C})$  is the length of the C–O bond.  $\angle(\text{O}-\text{C}-\text{H})$  and  $\angle(\text{Ag}_{\text{nor}}-\text{O}-\text{C})$  are, respectively, the angle between the CO and CH bonds and the angle of CO bond with respect to the surface normal (see Fig. 3.  $q(\text{adsorbate})$  is the total charge on the adsorbate in a.u. computed by Natural Population Analysis [47]. Frequencies are in  $\text{cm}^{-1}$

Ag(111)	Top	Top tilted	Bridge	Bridge tilted	hcp	fcc	Experimental
$E_a^a/\text{kJ mol}^{-1}$	−103.3	−124.8	−138.1	−144.7	−151.0	−178.5	
$d(\text{O}-\text{Ag}_{\text{surf}})/\text{Å}$	2.141	2.177	1.720	1.746	1.614	1.586	
$d(\text{O}-\text{Ag}_{\text{nm}})/\text{Å}$	2.141	2.177	2.247	2.267	2.321	2.302	
$d(\text{O}-\text{C})/\text{Å}$	1.372	1.365	1.401	1.406	1.409	1.404	
$\angle(\text{O}-\text{C}-\text{H})^\circ$	113.4	113.7	112.0	112.2	111.7	111.8	
$\angle(\text{Ag}_{\text{nor}}-\text{O}-\text{C})^\circ$	0.0	55.3	0.0	30.2	0.0	0.0	0.0 <sup>b</sup>
$q(\text{adsorbate})$	−0.81	−0.73	−0.74	−0.72	−0.73	−0.75	
$\nu_{\text{as}}(\text{CH}_3)$	2820	2835	2868	2853	2874	2871	
$\nu_{\text{as}}(\text{CH}_3)$	2820	2757	2859	2872	2869	2870	
$\nu_{\text{s}}(\text{CH}_3)$	2804	2803	2820	2819	2823	2825	2792 <sup>b</sup>
$\delta_{\text{as}}(\text{CH}_3)$	1435	1427	1452	1448	1454	1456	
$\delta_{\text{as}}(\text{CH}_3)$	1435	1377	1444	1450	1453	1447	
$\delta_{\text{s}}(\text{CH}_3)$	1440	1410	1441	1440	1440	1440	1432 <sup>b</sup>
$\rho(\text{CH}_3)$	1116	1092	1136	1135	1132	1138	
$\rho(\text{CH}_3)$	1115	1074	1119	1123	1137	1132	
$\nu(\text{CO})$	1144	1121	1082	1057	1061	1081	1048 <sup>b</sup>
$\nu(\text{OAg}_{\text{surf}})$	305	354	286	286	267	281	

<sup>a</sup> Negative values are exothermic.

<sup>b</sup> RAIRS values, Ref. [21].

atom is positioned above an M atom. These clusters, albeit small, were found previously to give a reasonable description of the copper surface. For example,  $\text{Cu}_7$  clusters were used in the study of adsorption of methoxy [37], formate [38], ethylene [39,40] and acetylene [40,41]. In order to test the validity of the clusters, a control test was performed for  $\text{CH}_3\text{O}^\cdot$  adsorbed on a fcc site of a  $\text{Cu}_{22}$  (14,8) cluster where seven metal atoms are treated with the LANL2DZ basis set and the other 15 metal atoms are treated with the LANL2MB basis set. The results obtained compare well with the data presented in Table 1. The Cu–O, C–O and C–H distances are 1.450, 1.416 and 1.099 Å, respectively. The O–C–H angle is 110.9°.

The  $\text{CH}_3\text{O}^\cdot$  geometry was totally optimized except the C–H bond length which was found previously [37] to be almost unchanged for methoxy radical adsorption on the different sites of the M(111) surfaces.

Previous work suggests that the methoxy radical adsorbs with the oxygen atom pointing towards the metal [17,21,31] and the C–O bond axis normal to the surface.

Throughout this work the three parameter hybrid method proposed by Becke [42] was used. It includes a mixture of Hartree–Fock (HF) and DFT exchange terms, associated with the gradient corrected correlation functional of Lee et al. [43]. The use of DFT allows for the inclusion of some correlation effects without incurring the huge costs of post-Hartree–Fock methods.

Only the valence electrons of the metal atoms were treated explicitly and the effects of the inner shell electrons ( $1s^2 2s^2 2p^6$ ) were included in the effective core potential (ECP) of Hay and Wadt [44,45]. To describe the oxygen, carbon and hydrogen atoms in the methoxy radical, the 6-31G\*\* basis set (double zeta plus p polarization functions in hydrogen atoms and d functions in oxygen and carbon atoms) was used.

Vibrational frequencies were obtained after optimization of the  $\text{CH}_3\text{O}^\cdot$  geometry adsorbed on  $\text{Cu}_7$  clusters. Again, this was done by DFT quantum calculation using the B3LYP method with the same basis sets as were used for the optimization procedure. The GAUSSIAN 94 [46] package was used.

Table 3

Methoxy adsorption properties for the different Au<sub>7</sub> clusters representing on-top, bridge and hollow sites.  $E_a$  is the methoxy adsorption energy,  $d(\text{O}-\text{Au}_{\text{surf}})$  is the perpendicular distance to the copper surface,  $d(\text{O}-\text{Au}_m)$  is the distance between the methoxy oxygen atom and the nearest Au atom(s) on the surface,  $d(\text{O}-\text{C})$  is the length of the C–O bond.  $\angle(\text{O}-\text{C}-\text{H})$  and  $\angle(\text{Au}_{\text{nor}}-\text{O}-\text{C})$  are, respectively, the angle between the CO and CH bonds and the angle of CO bond with respect to the surface normal (see Fig. 4).  $q(\text{adsorbate})$  is the total charge on the adsorbate in a.u. computed by Natural Population Analysis [47]. Frequencies are in  $\text{cm}^{-1}$

Au(111)	Top	Top tilted	Bridge	Bridge tilted	hcp	fcc	Experimental
$E_a^a/\text{kJ mol}^{-1}$	−6.9	−56.9	−45.4	−67.9	−66.1	−85.4	
$d(\text{O}-\text{Au}_{\text{surf}})/\text{Å}$	2.287	2.294	1.869	1.925	1.756	1.759	
$d(\text{O}-\text{Au}_m)/\text{Å}$	2.287	2.294	2.359	2.419	2.420	2.422	
$d(\text{O}-\text{C})/\text{Å}$	1.368	1.361	1.401	1.412	1.410	1.408	
$\angle(\text{O}-\text{C}-\text{H})^\circ$	113.1	113.6	111.8	111.9	111.4	111.4	
$\angle(\text{Au}_{\text{nor}}-\text{O}-\text{C})^\circ$	0.0	63.7	0.0	46.3	0.0	0.0	
$q(\text{adsorbate})$	−0.66	−0.59	−0.63	−0.57	−0.62	−0.65	
$\nu_{\text{as}}(\text{CH}_3)$	2812	2840	2871	2851	2879	2874	
$\nu_{\text{s}}(\text{CH}_3)$	2811	2740	2864	2839	2868	2877	
$\nu_{\text{s}}(\text{CH}_3)$	2804	2806	2822	2801	2820	2826	
$\delta_{\text{as}}(\text{CH}_3)$	1331	1413	1432	1454	1445	1450	
$\delta_{\text{as}}(\text{CH}_3)$	1332	1344	1448	1434	1451	1442	
$\delta_{\text{s}}(\text{CH}_3)$	1415	1373	1430	1428	1432	1437	
$\rho(\text{CH}_3)$	820	1065	1109	1134	1126	1122	
$\rho(\text{CH}_3)$	821	1039	1086	1113	1102	1082	
$\nu(\text{CO})$	1117	1110	1050	1011	1046	1062	
$\nu(\text{O}-\text{Au}_{\text{surf}})$	266	347	281	308	275	303	

<sup>a</sup> Negative values are exothermic.

### 3. Results

Tables 1–3 report the calculated adsorption energies as well as the equilibrium distances between oxygen and the (111) surface, between oxygen and the nearest metallic atom(s) on the (111) surface, and between oxygen and carbon; also shown in these tables is the O–C–H angle, and the angle between the normal to the metallic surface and the CO bond, as well as atomic charges and vibrational frequencies. The data are for adsorption of the methoxy radical on surfaces of copper (Table 1), silver (Table 2) and gold (Table 3).

For copper (Table 1), the calculated distance between oxygen and the nearest copper atom(s) ( $\text{O}-\text{Cu}_m$ ) is almost unaffected by which adsorption site is considered. However, for the top site, the  $\text{O}-\text{Cu}_{\text{surf}}$  distance is much higher than that obtained for adsorption on the other positions. The calculated oxygen to copper surface distance is higher than that obtained experimentally [15] ( $1.32 \pm 0.05$ ) for the Cu(111) surface. The agreement is better for the hollow sites (1.46–1.51 Å). In a previous work, Witko et al. [16,33] have found by means of ab initio HF for a

Cu<sub>25</sub> cluster an oxygen to copper surface distance of 1.47 Å for adsorption of methoxy on the fcc hollow site of the Cu(111) surface. The distance obtained by Witko et al. is very close to the value obtained in this work. The other  $d(\text{O}-\text{Cu}_{\text{surf}})$  for  $\text{CH}_3\text{O}^\cdot$  adsorbed on the top, bridge and hcp hollow sites are also very close, 1.89, 1.58 and 1.52 Å, respectively.

The reason for the higher calculated  $\text{O}-\text{Cu}_{\text{surf}}$  distance when compared with the experimental value of Ref. [15] seems to be due mainly to the absence of relaxation effects of the metal atoms in the theoretical works. The effects of relaxation were considered in the photoelectron diffraction study in both the  $z$  and  $xy$  directions. The  $z$  direction is the one that contains the O–C bond of the methoxy radical. The nearest-neighbor copper atoms are displaced from the other first layer copper atoms by  $0.07 \pm 0.05$  in the  $z$  direction and  $0.00 \pm 0.05$  in the  $xy$  direction. Therefore, we cannot compare directly the distance obtained with the experimental value but, still, they seem to agree well.

The adsorption energy is higher for the fcc three-hollow sites. For top and bridge positions the adsorption energy increases with the tilting of the C–O axis

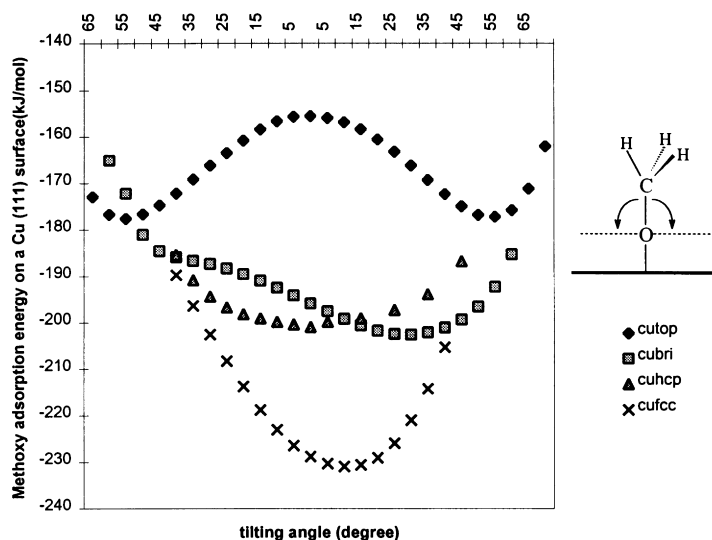


Fig. 2. Tilting effect for methoxy radical adsorbed on a Cu(111) surface. There is no optimization of the  $\text{CH}_3\text{O}$  geometry. Negative adsorption energy values are exothermic.

and the adsorption energy reaches a maximum for the top site when the C–O axis is bent by  $53.1^\circ$  with respect to the normal to the copper surface and for the bridge position when this angle is equal to  $30.1^\circ$ . For the hollow sites the tilting effect upon the stabilization is smaller than the effect observed for the top and bridge sites and stabilization is observed only for

small tilt angles. For larger tilt there is a high destabilization (see Fig. 2).

For adsorption on a top site, the results plotted in Fig. 2 show that there is a stabilization effect that reaches a maximum value when the C–O axis is tilted away from the surface normal by about  $55^\circ$  and it is unchanged if one or two hydrogen atoms approach the

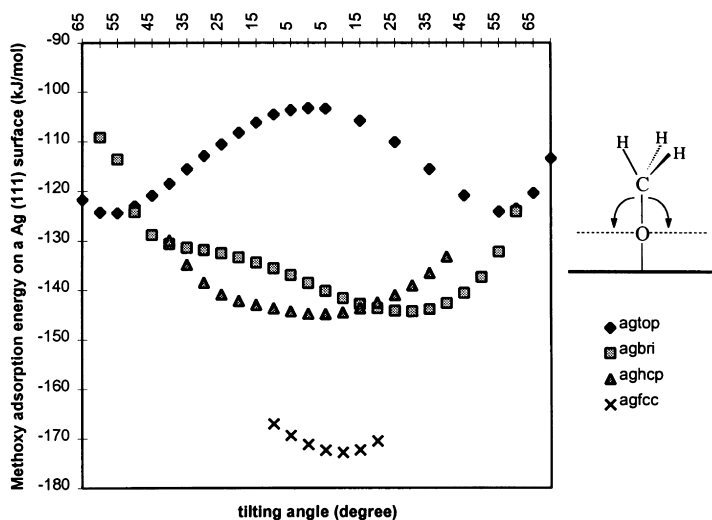


Fig. 3. Tilting effect for methoxy radical adsorbed on an Ag(111) surface. There is no optimization of the  $\text{CH}_3\text{O}$  geometry. Negative adsorption energy values are exothermic.

surface. The energy stabilization is  $\approx 20$  kJ/mol. For adsorption on a bridge site, there is stabilization ( $\approx 8$  kJ/mol) only if the C–O axis is tilted from the surface normal with the two hydrogen atoms approaching the copper surface with a tilting angle of about  $30^\circ$ . For the hollow sites, the most stable position is with methoxy radical C–O axis normal to the surface on the hcp position and very close to the normal for the fcc position.

The internal geometry of the  $C_{3v}$  methoxy radical is very different for the adsorption on the top sites when compared with the other sites.  $d(O-C)$  is 1.375 and 1.368 Å for upright and tilted adsorption on this site while on the other sites the O–C bond length is larger (1.395–1.414 Å). The same behavior is found for the O–C–H angle. For adsorption on top sites this angle is ca.  $113^\circ$  compared with  $111^\circ$  for bridge and hollow sites.

The methoxy total and atomic charges calculated by natural population analysis (NPA) [47] are very similar for the different sites studied.

NPA charges for the hydrogen atoms are more positive when the number of nearest neighbors is higher than one. Charge on the oxygen and carbon atoms are almost the same for all the sites considered and the total charge for the methoxy radical remains ca  $-0.75e$ .

The calculated vibrational frequencies are in good agreement with available experimental data. Frequencies involving the  $CH_3$  group do not vary much with the adsorption site. Comparison with experimental data show that the maximum displacement occurs for adsorption at the top site. Probably, this different behavior is caused by the larger oxygen–copper surface distance when compared with the bridge and the three hollow sites. The hydrogen atoms are in this case too far from the surface and there is a minor effect of the surface and they can vibrate more freely. We can conclude that there is some interference of the copper surface in the carbon–hydrogen bonds. Witko et al. [16,33] have assigned the EELS band at  $2888\text{ cm}^{-1}$  to the  $2\delta_{as}(CH_3)$  mode and the one at  $2922\text{ cm}^{-1}$  to the  $\nu_{as}(CH_3)$  mode. From our results it seems that the band at  $2888\text{ cm}^{-1}$  is due to the  $CH_3$  anti-symmetric stretching and the band at  $2922\text{ cm}^{-1}$  arises because of the  $CH_3$  anti-symmetric deformation; the calculated  $\delta_{as}(CH_3)$  is  $1460\text{ cm}^{-1}$ , approximately. The two calculated  $\nu_{as}(CH_3)$  frequencies are

very close and that is the reason why only one band is observed experimentally. The same happens for the two  $\delta_{as}(CH_3)$  and for the two  $\rho(CH_3)$  calculated frequencies and the consequence is that there is only one experimental band for each case.

The CO vibrational frequencies obtained for the adsorption on top sites are higher than the ones obtained for the other adsorption positions. The calculated CO vibrational frequency for the four different sites does not agree as well as the ones obtained for the modes involving the methyl groups, perhaps because of the smaller value found for the C–O bond distance when compared with the experimental one (1.42 Å) [15].

The general behavior of the properties of methoxy radical adsorbed on the silver surface (see Table 2) are similar to those observed for the copper surface. The adsorption energy is smaller and the distances from the oxygen atom to the surface for the different adsorption sites are higher. Again, the most stable site is the fcc hollow and methoxy is most stabilized on the top and bridge sites if the C–O axis is tilted away from the surface normal by  $55.3$  and  $30.2^\circ$ , respectively. The variation of the adsorption energy with the tilting angle of the C–O axis is shown in Fig. 3. The adsorption energy is lowered by approximately 20 kJ/mol for  $CH_3O^\cdot$  adsorbed tilted on the top site. At the hollow sites the most stable geometry is found with the C–O axis perpendicular to the surface. For the hollow sites, the oxygen to silver surface distance is about 1.60 Å. The methoxy radical internal geometry is very similar to the one observed for copper. The carbon–oxygen distance is smaller for adsorption on the top site (about 1.37 Å) than for adsorption on the other sites (1.40–1.41). The NPA charges are also similar to those observed for adsorption on copper. The vibrational frequencies are in good agreement with the experimental data. In general, they are higher than the experimental values by approximately  $20\text{ cm}^{-1}$ . The absence of anti-symmetric bands in the experimental (RAIRS) results probably means that the methoxy radical is less tilted when adsorbed on the silver surface than on the copper surface. The C–O stretching frequencies, obtained theoretically for adsorption on the different sites of the silver surface, are very similar to the experimental value. When compared with the behavior for adsorption on Cu(111) this probably means that the C–O bond

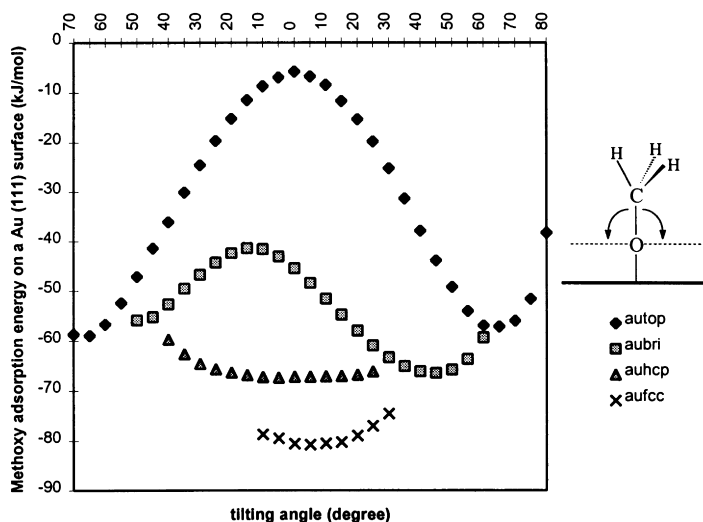


Fig. 4. Tilting effect for methoxy radical adsorbed on an Au(111) surface. There is no optimization of the  $\text{CH}_3\text{O}$  geometry. Negative adsorption energy values are exothermic.

length found (1.40–1.41 Å) is very close to the real bond length for methoxy adsorption on the Ag(111) surface. The oxygen–metallic surface stretching frequency falls within the interval  $267\text{--}286\text{ cm}^{-1}$ . The values obtained for adsorption on the top site, as those obtained for adsorption on copper, are far from the frequency values obtained for the bridge and hollow sites.

In the gold surface (see Table 3), the  $\text{CH}_3\text{O}$  adsorption on the bridge site is similar in terms of energy to the adsorption on the hcp hollow site. The distance of the oxygen atom to the surface is higher than that observed for copper and silver and this causes a lowering in the adsorption energy. This higher methoxy–surface distance causes the tilting angle for adsorption on the top and on the bridge site to be higher than for copper or silver. The most stable position is with a CO tilt angle of  $63.7^\circ$  for adsorption on a top site and  $46.3^\circ$  for adsorption on a bridge site (see Fig. 4). This CO tilting stabilizes the methoxy radical by  $\sim 50\text{ kJ/mol}$  for adsorption on the top site and by more than  $20\text{ kJ/mol}$  for adsorption on the bridge site. The charge transfer is smaller than that observed for the other two surfaces ( $\approx 0.6e$ ). The vibrational frequencies are very similar to the ones obtained for adsorption on the silver surface. The O–Au surface stretching frequency lies in the interval  $270\text{--}308\text{ cm}^{-1}$ .

The variation of the dipole moment with the

distance of the oxygen atom to the metal surface is plotted in Fig. 5. In this figure only the dipole moment variation for  $\text{CH}_3\text{O}$  adsorbed on the most favorable site, fcc is plotted. By consideration of the derivative with respect to the  $\text{OM}_{\text{surf}}$  distance, together with the NPA charges, more information may be obtained about the type of bonding of methoxy radical to the copper surface. This technique is based on a simple model [48–52]. For an ionic molecule represented by two point charges  $+q$  and  $-q$  with the negative

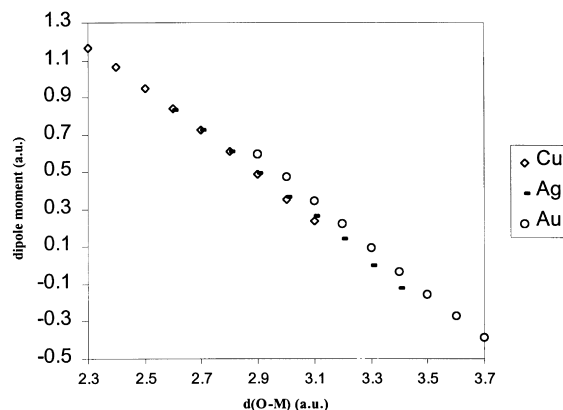


Fig. 5. Calculated dipole moment for the methoxy radical adsorbed on the Cu(111), Ag(111) and Au(111) fcc hollow sites as a function of the methoxy oxygen atom–copper surface distance.

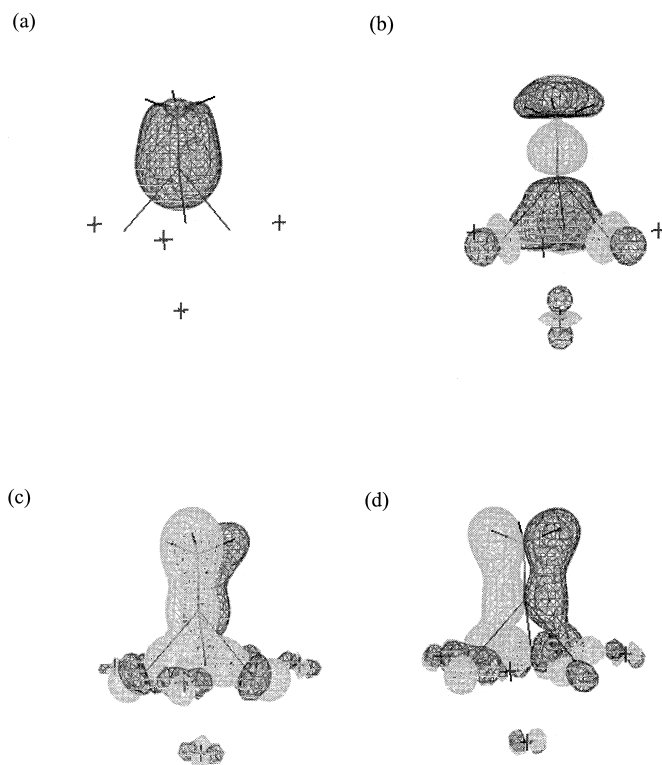


Fig. 6. Main binding molecular orbitals for methoxy adsorbed on an hcp hollow on the Cu(111) surface. Dark gray represents an isocontour for  $\psi = +0.05$  and light gray an isocontour for  $\psi = -0.05$ . The gOpenMol graphical interface [53] was used. (a)  $\sigma$  (C–O); (b)  $\sigma$  (O–Cu<sub>surf</sub>); (c)  $\pi$  (O–Cu<sub>surf</sub>) and (d)  $\pi$  (O–Cu<sub>surf</sub>).

charge on the positive  $z$  axis, the dipole moment is  $\mu_z = -q \times l$ , where  $l$  is the distance between the two point charges. For a fully ionic molecule with  $q = 1$ ,  $d\mu/dl = -1$  the curve is a straight line. In the case of ionic bonding, therefore, the slope is expected to be large and the curvature,  $d^2\mu/dl^2$ , is expected to be small. The calculated slope for  $\text{CH}_3\text{O}^\cdot$  adsorbed on the Cu(111) fcc hollow site is  $-1.17$ . The large slope and the linearity of dipole moment (as a function of the O–Cu distance) are indicative of a very ionic O–Cu bond. This bonding of the methoxy radical oxygen atom to the surface involves several copper atoms and the number of metal atoms involved increases from the top site to the hollow sites. The main bonding molecular orbitals formed by the oxygen atom for adsorption of the methoxy radical on hollow sites are shown in Fig. 6. The bonding scheme is similar for the different adsorption sites. The oxygen 2p atomic orbitals interact with the 3d

orbitals of the copper atoms and three different molecular orbitals are formed (one  $\sigma$  and two  $\pi$ ). The oxygen 2s atomic orbital interacts with the carbon atom to form the C–O bonding. For upright adsorption of methoxy radical on a top site the bonding scheme is less  $\pi$  bonding. The  $\pi$  character increases from 1- to 3-fold adsorption sites and it must be correlated with a higher adsorption energy for adsorption on hollow positions. Fig. 5 also shows the variation of the dipole moment with the distance of the oxygen atom to the Ag(111) and Au(111) surfaces. The slope obtained is very similar to that obtained for adsorption on the copper surface. The calculated slope is  $-1.19$  and  $-1.22$  a.u. for silver and gold, respectively. The binding scheme is very similar to the one reported for copper. Its nature is ionic with a charge transfer from the metal surface to  $\text{CH}_3\text{O}^\cdot$  of about  $0.75e$  on both surfaces.

Fig. 7 reports the effect in the adsorption energy of

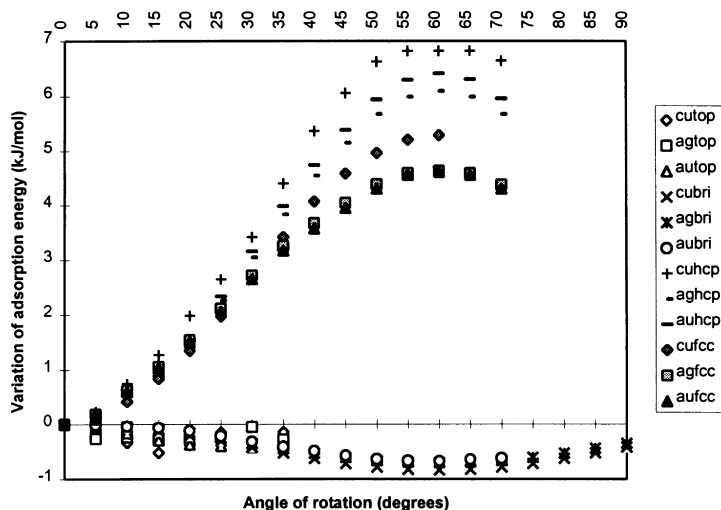


Fig. 7. Methyl group rotation for methoxy adsorbed upright on top, bridge and hollow sites of copper, silver and gold(111) surfaces.

rotating the methyl group of the methoxy radical. These results are for the adsorbed upright species. The rotation of the methyl group has a minimal influence in the adsorption energy and it is higher (by about 7 kJ/mol) for adsorption on hollow sites where it was calculated a smaller oxygen to surface distance. For bridge and top sites the energy variation during rotation is less than 1 kJ/mol. The methyl group is supposed to rotate freely above the metallic surfaces considered.

#### 4. Conclusions

The density functional theory results reported here for methoxy radical adsorbed on copper, silver and gold(111) surfaces show that the adsorbate is stable at all the different sites on these surfaces. At the preferred adsorption geometry of methoxy radical on three-hollow sites, it has its O atom pointing towards the surface and the C–O axis approximately perpendicular to the surface. On the top and bridge adsorption positions, the adsorption energy is higher if the C–O axis is tilted from the surface normal with one or two hydrogen atoms approaching the surface for adsorption on 1-fold sites or with two hydrogen atoms approaching the surface for adsorption on 2-fold sites. The following sequence of stability is obtained for methoxy adsorbed on the (111) metallic

surfaces considered, top < bridge < hcp < fcc, but for the gold surface, the adsorption energies on the bridge and on the hcp hollow sites are very similar. The adsorption energy decreases in the copper group from copper to gold. For upright adsorption, the methyl group rotation energy barrier is minimal with the highest value ( $\sim 7.0$  kJ/mol) being found for hollow sites where the hydrogen atoms are much closer to the surface.

Since the computed results compare well with the experimental data (for copper and silver surfaces) and with theoretical calculations (on a copper surface), it is thought that the results now presented for  $\text{CH}_3\text{O}$  adsorption on the Au(111) surface give a good estimate of the true values. Furthermore, the results obtained for adsorption on the copper surface compare well with the data obtained for a much larger ( $\text{Cu}_{22}$ ) cluster.

The bonding of the methoxy radical on the three surfaces considered is essentially ionic with a quite large charge transfer (0.6–0.8 $e$ ) from the metallic surface to the adsorbate. The atomic orbitals involved on the bonding scheme are the oxygen p orbitals and the d orbitals from the metallic atoms and one  $\sigma$  bond and two  $\pi$  bonds are formed. The  $\pi$  character increases from adsorption on 1-fold sites to adsorption on 3-fold sites. Despite this similar binding scheme, the copper surface stabilizes more efficiently the methoxy radical. This stronger interaction observed

on copper is due to the smaller calculated O–surface distance and to the greater interaction between the adsorbate and the surface. The calculated adsorbate charges are higher when the methoxy radical is adsorbed on copper. Also, despite the similarity between the Ag–Ag and Au–Au distances, an higher adsorption energy and a smaller O–M distance when the radical is adsorbed on the silver surface is calculated. This effect is shown also in the calculated adsorbate charge which decreases from copper to gold.

The calculated vibrational frequencies agree well with the available experimental data. The larger displacement is observed for the C–O stretching mode because of the smaller C–O bond length obtained theoretically.

### Acknowledgements

Financial support from the Fundação para a Ciência e Tecnologia (Lisbon) and project PRAXIS/PCEX/C/QUI/61/96 is acknowledged. JRBG thanks PRAXIS for a doctoral scholarship (BD/5522/95).

### References

- [1] R. Ryberg, Phys. Rev. Lett. 49 (1982) 1579.
- [2] R. Ryberg, Phys. Rev. B 31 (1985) 2545.
- [3] I.E. Wachs, R. Madix, J. Catal. 53 (1978) 208.
- [4] H.E. Dastoor, P. Gardner, D.A. King, Chem. Phys. Lett. 209 (1993) 493.
- [5] N.D. Shinn, Surf. Sci. 278 (1992) 157.
- [6] J.S. Huberty, R.J. Madix, Surf. Sci. 360 (1996) 144.
- [7] S.R. Bare, J.A. Stroschio, W. Ho, Surf. Sci. 150 (1985) 399.
- [8] R. Zenobi, J. Xu, J.T. Yates Jr., B.N.J. Persson, A.I. Volotkin, Chem. Phys. Lett. 208 (1993) 414.
- [9] M.A. Karolewski, R.G. Cavell, Surf. Sci. 344 (1995) 74.
- [10] T.H. Ellis, H. Wang, Langmuir 10 (1994) 4083.
- [11] J.P. Camplin, E.M. McCash, Surf. Sci. 360 (1996) 229.
- [12] A.F. Carley, P.R. Davies, G.G. Mariotti, S. Read, Surf. Sci. 364 (1996) L525.
- [13] C. Barnes, P. Pudney, Q. Guo, M. Bowker, J. Chem. Soc. Faraday Trans. 86 (1990) 12 693.
- [14] S.M. Francis, F.M. Leibsle, S. Haq, N. Xiang, M. Bowker, Surf. Sci. 315 (1994) 284.
- [15] P. Hofmann, K.-M. Schindler, S. Bao, V. Fritzche, D.E. Ricken, A.M. Bradshaw, D.F. Woodruff, Surf. Sci. 304 (1994) 74.
- [16] M. Witko, K. Hermann, D. Ricken, W. Stenzel, H. Conrad, A.M. Bradshaw, Chem. Phys. 177 (1993) 363.
- [17] A.V. de Carvalho, M.C. Asensio, D.P. Woodruff, Surf. Sci. 273 (1992) 381.
- [18] M. Chesters, E.M. McCash, Spectrochim. Acta 43A (1987) 1625.
- [19] Q. Dai, A.J. Gellman, Surf. Sci. 102 (1991) 271.
- [20] I.E. Wachs, R.J. Madix, Surf. Sci. 76 (1978) 351.
- [21] W.S. Sim, P. Gardner, D.A. King, J. Phys. Chem. 99 (1995) 16 002.
- [22] D.A. Outka, R.J. Madix, J. Am. Chem. Soc. 109 (1987) 1708.
- [23] N. Hartmann, F. Esch, R. Imbihl, Surf. Sci. 297 (1993) 175.
- [24] J.-J. Chen, Z.-C. Jiang, Y. Zhou, B.R. Chakraborty, N. Wironograd, Surf. Sci. 328 (1995) 248.
- [25] N. Kizhakevarium, E.M. Stuve, Surf. Sci. 286 (1993) 246.
- [26] J. Wang, M.A. de Angelis, D. Zaikos, M. Setiadi, R.I. Masel, Surf. Sci. 318 (1994) 307.
- [27] E.I. Ko, R.J. Madix, Surf. Sci. 112 (1981) 373.
- [28] M.K. Weldon, P. Uvdal, C.M. Friend, J.G. Serafin, J. Chem. Phys. 103 (1995) 5075.
- [29] M. Kerkar, A.B. Hayden, D.P. Woodruff, M. Kadodwala, R.G. Jones, J. Phys. Condens. Matter 4 (1992) 5043.
- [30] M. Bader, A. Puschmann, J. Haase, Phys. Rev. B 33 (1986) 7336.
- [31] E. Holub-Krappe, K.C. Prince, K. Horn, D.P. Woodruff, Surf. Sci. 173 (1986) 176.
- [32] H. Yang, J.L. Whitten, C.M. Friend, Surf. Sci. 313 (1994) 295.
- [33] M. Witko, K. Hermann, J. Chem. Phys. 101 (1994) 10 173.
- [34] D.A. Outka, R.J. Madix, J. Stoehr, Surf. Sci. 164 (1985) 235.
- [35] R. Ryberg, Chem. Phys. Lett. 83 (1981) 423.
- [36] T. Lindner, J. Somers, A.M. Bradshaw, A.L.D. Kilcoyne, D.P. Woodruff, Surf. Sci. 203 (1988) 333.
- [37] J.R.B. Gomes, J.A.N.F. Gomes, J. Mol. Struct. (Theochem) 463 (1999) 163.
- [38] J.R.B. Gomes, J.A.N.F. Gomes, Surf. Sci. 432 (1999) 279.
- [39] K. Hermann, M. Witko, A. Michalak, Z. Phys. Chem. 197 (1996) 219.
- [40] A. Michalak, M. Witko, K. Hermann, J. Mol. Catal. A: Chem. 119 (1997) 213.
- [41] A. Clotet, G. Pacchioni, Surf. Sci. 346 (1996) 91.
- [42] A.D. Becke, J. Chem. Phys. 98 (1993) 5648.
- [43] C. Lee, W. Yang, R.G. Parr, Phys. Rev. B 37 (1980) 785.
- [44] P.J. Hay, W.R. Wadt, J. Chem. Phys. 82 (1985) 270.
- [45] P.J. Hay, W.R. Wadt, J. Chem. Phys. 82 (1985) 299.
- [46] M.J. Frisch, G.W. Trucks, H.B. Schlegel, P.M.W. Gill, B.G. Johnson, M.A. Robb, J.R. Cheeseman, T. Keith, G.A. Petersson, J.A. Montgomery, K. Raghavachari, M.A. Al-Laham, V.G. Zakrzewski, J.V. Ortiz, J.B. Foresman, J. Cioslowski, B.B. Stefanov, A. Nanayakkara, M. Challacombe, C.Y. Peng, P.Y. Ayala, W. Chen, M.W. Wong, J.L. Andres, E.S. Replogle, R. Gomperts, R.L. Martin, D.J. Fox, J.S. Binkley, D.J. Defrees, J. Baker, J.P. Stewart, M. Head-Gordon, C. Gonzalez, J.A. Pople, GAUSSIAN 94, Revision D.4, Gaussian, Inc., Pittsburgh, PA, 1995.
- [47] E.D. Glendening, A.E. Reed, J.E. Carpenter, F. Weinhold, NBO version 3.1, Program included in the GAUSSIAN 94 package.
- [48] C.J. Nelin, P.S. Bagus, M.R. Philpott, J. Chem. Phys. 87 (1987) 2170.

- [49] P.S. Bagus, G. Pacchioni, M.R. Philpott, *J. Chem. Phys.* 90 (1989) 4287.
- [50] G. Pacchioni, P.S. Bagus, M.R. Philpott, *Physica D* 12 (1989) 543.
- [51] G. Pacchioni, P.S. Bagus, M.R. Philpott, C.J. Nelin, *Int. J. Quant. Chem.* 38 (1990) 675.
- [52] P.S. Bagus, F. Illas, *Phys. Rev. B* 42 (1990) 10 852.
- [53] gOpenMol, Version 1.00, Leif Laaksonen, Center for Scientific Computing, Espoo, Finland, 1997.